Chapter 4

TOWARDS SURFACE PATTERNING USING PHYSISORBED MONOLAYERS AS MASKS

4.1 Overview

Many small organic molecules in solution spontaneously form highly ordered physisorbed monolayers on surfaces. The monolayers are readily observable under ambient laboratory conditions and are highly structured with feature sizes on the scale of a small molecule. A single monolayer domain can cover a relatively large surface area, and the structure of the monolayer can leave areas of the underlying surface exposed. Thus a physisorbed monolayer may be useful as a mask in an inexpensive surface patterning technique that would be capable of producing feature sizes on the order of a few nanometers. In order to accomplish such patterning, a physisorbed monolayer that incorporates pores in its structure would be used to mask a surface while an additional species that reacts chemically with the exposed areas of the surface is added to the overlying solution. The surface could then be cleaned, removing the physisorbed masking monolayer, and exposed again to other surface-reactive species. This procedure would leave a chemical pattern with single nanometer-scale features on the surface. Gold is a promising substrate for such patterning because, although it is relatively inert and thus will not corrode or degrade under ambient laboratory conditions, it is known to react with and bond to alkylthiols. This chapter describes an approach to patterning gold surfaces using physisorbed monolayer masks and thiol chemistry. Gold surface preparation methods are described and molecular candidates for mask formation are discussed. Significant challenges to obtaining stable masking monolayers on gold surfaces were met and are discussed in detail. Electrochemical techniques offer a promising approach to meeting these challenges.

4.2 Introduction

Stable, highly ordered monolayers are spontaneously formed on a number of surfaces by long-chain normal and substituted alkanes and aromatics in solution.[1] These surfaces include graphite, molybdenum disulfide, and tungsten disulfide.[2] The primary source of the force driving monolayer formation is favorable intermolecular interactions such as van der Waals forces and hydrogen bond formation.[3–7] The molecules do not bond to the surface and are free to exchange with other molecules in the overlying solution. When an atomically flat surface such as highly oriented pyrolytic graphite (HOPG) is used as a substrate, a scanning tunneling microscope (STM) can be employed to observe the monolayers under standard laboratory conditions.[8] The physisorbed monolayers cover the entire adsorbent surface and the molecules form monolayers composed of ordered domains with lamellar structures. Many domains can cover the surface to give a two-dimensional structure analogous to that of polycrystalline solids. The surface area covered by a single domain reflects the overall stability of the monolayer, as larger domains reduce the number of unstable domain boundaries in the monolayer. A single ordered domain can easily cover an area greater than 10,000 square nanometers, as seen in Figure 4.1, and it may be possible to increase the average domain size through a thermal annealing process. The ability to produce reasonably large ordered domains with features on the nanometer scale under ambient conditions suggests potential for the use of physisorbed molecular monolayers as templates for surface patterning.

One approach to surface patterning using physisorbed monolayer templates is to employ the monolayer as a surface mask in a manner analogous to traditional photolithographic methods. The masking monolayer would be selected for its ability to form a stable structure that incorporates pores which leave regions of the underlying surface exposed. After the monolayer forms on the surface, a species known to react controllably with the surface would be added to the overlying solution resulting in a surface reaction only in the areas left exposed by the monolayer structure. The surface could then be cleaned to remove the masking monolayer and exposed again to a different species that would react only at the newly uncovered regions of the surface. This sequence would produce a chemically patterned surface with features on the single nanometer scale. Such a surface could be useful for catalysis applications and as a way to tether nanoparticles to a surface in an ordered array, which would allow studies of the electrochemical properties of single nanoparticles.

HOPG is by far the most widely used substrate in studies of self-assembled physisorbed monolayers. This is because HOPG is conductive, is inert under standard laboratory conditions and has a layered structure that allows the easy preparation of an atomically flat surface. The inert nature of HOPG, however, is extremely problematic if one wishes to pattern the surface regions left exposed by a physisorbed monolayer. Thus, in order to pursue this approach to surface patterning, it is necessary to employ a surface that is more amenable to chemical modification. Gold has also been used successfully as a substrate in STM studies and is a promising candidate for a substrate surface for this approach to surface patterning. The gold surface does not significantly corrode or degrade under laboratory conditions and physisorbed monolayer structures similar to those formed on HOPG have been observed on the reconstructed Au(111) surface.[9] Although the gold surface is relatively inert under standard laboratory conditions, it is known to react with alkyl sulfides, disulfides, and other soft nucleophiles.[10] Gold may therefore prove to be a useful substrate for a demonstration of surface patterning using physisorbed monolayers as masks.

A number of methods have been used to prepare atomically flat gold surfaces. The simplest procedure involves the deposition of gold onto a flat surface such as mica, silicon, or glass. The surface is then flame annealed. The gold can be deposited by either evaporation or sputtering. Gold surfaces with terraces averaging 6300 Å in width have been prepared using this method and the surfaces that resulted were exclusively Au (111).[11] A number of researchers have successfully prepared gold surfaces using similar methods.[12–14] Gold-coated mica substrates are commercially available and have been used successfully in an STM study of liquid crystals.[15] Molecular Imaging, Inc., is one such supplier and recommends annealing the surface in a hydrogen flame prior to use. Other commonly used methods of gold surface preparation for STM are adaptations of the method for the preparation of monocrystalline platinum electrodes that was detailed by Clavilier et al.[16] These methods involve the use of a single-crystalline gold bead that is purchased or obtained by melting a pure gold wire using a hydrogen-oxygen flame. The resulting bead is etched using either aqua regia or piranha solution, cut along the desired direction, and annealed with a hydrogen flame.[17–19]

Although HOPG is by far the most commonly used substrate for STM studies of physisorbed monolayers, a number of researchers have published STM images of monolayers on the reconstructed Au(111) surface. Monolayers formed at the interface of gold and the neat normal alkanes with carbon chain lengths from 12 through 17 have been imaged using an STM.[9,17] STM images of a monolayer of hexatriacontane, $C_{36}H_{74}$, adsorbed onto gold from a dodecane solution have also been published.[20] STM images of physisorbed monolayers at the interface between gold and other liquids have been published more recently. These liquids include the following: normal alkanes with even carbon chain lengths between 28 and 50 dissolved in tetradecane;[21] selected normal alkanes with carbon chain lengths of 14–38 either neat or dissolved in tetradecane;[22] and selected primary alcohols with chain lengths from 10–30 either neat or dissolved in tetradecane.[23] The monolayers observed on gold surfaces are similar to those formed on HOPG in that the molecules are arranged in lamellate domains on the surface, and in many cases a single ordered monolayer domain covers an entire Au(111) terrace.[9] STM studies involving the potential-dependent physisorption of molecules onto gold surfaces from aqueous solutions have also been published. He et al.[18] observed potential-dependent adsorption of a monolayer of hexadecane from a 0.1 M $HClO_4$ solution. These monolayers formed after the reconstruction of the gold surface was lifted by a potential step and were only stable in the potential range of 0.15–0.55 V_{SCE}. Researchers have also observed ordered monolayers of 1,3,5-benzenetricarboxylic acid, or trimesic acid (TMA), on gold surfaces in 0.1 M $HClO_4$.[24,25] Xu et al.[19] obtained STM images of a monolayer of a phospholipid on gold.

This work was also performed using an overlying $HClO_4$ solution and the structure of the monolayer was observed to change throughout the course of the experiment.

Images of physisorbed monolayers on HOPG surfaces which incorporate openings into their structure have already been published.[26,27] Some of the molecules which have been shown to incorporate spaces into their monolayer structures include liquid crystals and some derivatives of 1,3-disubstituted benzene, dehydrobenzo[12]annulene, and 1,3,5-trisubstituted benzene. Porous monolayers have also been observed to form on Au(111) and Ag(111) surfaces.[15,28,29]

It has been well established that the simple exposure of a gold surface to a solution of alkyl thiols in ethanol results in the attachment of a single molecular layer of the thiols to the gold surface.[10] The thiols act as soft nucleophiles and attach to the gold surface as metal thiolates (RS^-M^+).[30] The properties of the resulting surface can be tuned by altering the functional group on the tail of the thiol molecule.[31] The gold–thiol chemistry has also been demonstrated using solutions of thiols and disulfides in acetonitrile, isooctane, and hexadecane.[30]

The energy associated with the chemisorption of a thiolate on gold is on the order of tens of kcal mol^{-1}.[32] The energy associated with the physisorption of alkanes on gold is currently unknown; the values that have been reported for adsorption of alkanes on graphite are similar to those for the chemisorption of thiolates on gold.[2] However, it is possible that the heat of adsorption for alkanes on gold may be much less (~ 10–20 kcal mol^{-1}) than the value for adsorption on graphite. Thus, it may be necessary to arrest the chemisorption of thiolate onto the gold surface and to select for combinations of strongly physisorbed alkanes and weakly chemisorbed thiols. Both of the adsorption mechanisms derive a measure of stability from van der Waals interactions between adjacent alkane chains, and the strength of this interaction increases with the length of the alkane chain.[10,33] Thus it may be possible to decrease or slow the chemisorption of the thiolate by selecting thiols with relatively short or branched alkyl chains. Additional approaches to controlling the adsorption of the thiol may involve the removal of the thiol from the overlying solution after a limited period of exposure to the gold surface. It should be possible to accomplish this through the addition of an additional reagent to the overlying solution. Alkane thiols are weak acids with pK_a values near 10.6, and are easily oxidized.[34] The alkane thiolate species which attaches to the gold surface is a nucleophile and thus can form bonds with electron-deficient carbon atoms.[35] These properties suggest ways to remove excess thiols from the overlying solution in order to arrest the reaction at the surface and caution that the monolayer template must be carefully chosen so that the molecules which comprise it do not contain groups that are likely to react with the thiols.

4.3 Preparation of Gold Surfaces

4.3.1 Experimental Details

Three general approaches to the preparation of atomically flat gold surfaces were explored: evaporation of gold onto a flat substrate material; preparation of a crystalline gold bead; and direct sample purchase from a supplier. Highly oriented pyrolytic graphite (grade SPI-1) and 12 mm mica disks (grade V-1) were obtained from Structure Probe, Inc., and used as substrates for the evaporated gold samples. The substrates were secured in an inverted configuration above the source in an evaporator chamber using double-sided carbon tape suitable for high vacuum applications. The evaporator was an Edwards Coating System E306A equipped with a bell jar from Huntington Labs, Inc. Gold was evaporated onto the substrates at a rate of 20 Å s^{-1} to a final thickness of ~ 800 nm. The gold source for the evaporation was a 99.999% pure 0.25 mm wire from Alfa Aesar. For a few samples, a thin layer of chromium (99.996% pure from Alfa Aesar) was evaporated onto the substrates as an adhesion layer before the gold evaporation. The samples were annealed for ~ 5 minutes in a pure hydrogen flame about 30 minutes prior to STM imaging. A crystalline gold bead ~ 2.5 mm in diameter was prepared by melting a clean 99.999% pure 1 mm gold wire from Alfa Aesar in a gas-oxygen flame. The bead was then etched briefly in aqua regia and rinsed with pure water. Two commercially prepared 1 cm x 1.1 cm samples of gold on mica were obtained from Molecular Imaging, Inc. and were annealed for ~ 1 minute in a hydrogen flame before imaging. STM imaging of the samples was performed under ambient conditions using fresh, mechanically cut 80:20 Pt/Ir tips. Images were collected using a Digital Instruments (Veeco) Nanoscope III STM controlled by Nanoscope software version 5.12r2. Each image consisted of 512 sample lines. A real-time plane-fitting function was applied to the images during scanning, but no further image corrections were performed. A metallic clip that is used to hold samples in place on the STM was used to make electrical contact to the mica-backed samples and to clamp the samples to the stage during imaging.

4.3.2 Results

Figure 4.2 presents STM images of the gold samples prepared by evaporation in our laboratory. STM images of HOPG and Si(111) are included for comparison purposes and the images are presented on the same scale to facilitate a direct comparison of gross surface roughness. From these images, it is clear that the commercially prepared samples of gold on mica were smoother than the evaporated samples prepared in our laboratory. It is also clear from the images in Figure 4.2 that annealing the laboratory-prepared evaporated gold samples significantly increased the crystallinity of the samples and reduced the roughness of the surface. Paradoxically, the annealing step did appear to roughen the surface on the scale visible with a light microscope. The laboratory-prepared samples were very easily damaged by scratching and in some cases significant portions of the surface were removed by accidental contact. The samples prepared using chromium adhesion layers were damaged as easily as those prepared by evaporating gold directly onto the substrate.

STM images exhibiting atomic-scale resolution were obtained for both the commercial and laboratory-prepared samples. These images are presented in Figure 4.3 and show a hexagonal array of atoms with a lattice spacing measured as 2.8–2.9 Å. STM images of the gold bead were not obtained as it was apparent that contacting and mounting such a small sample would prove difficult. It was expected that this difficulty would be exacerbated during later stages of the experiment when it would be necessary to mount the sample inside a liquid cell.

4.3.3 Discussion

The commercially prepared samples of gold evaporated onto mica exhibited the smoothest surfaces both before and after annealing. The STM images of these samples showed evidence of a polycrystalline surface and flat terraces with a wide size range. The smaller terraces were ~ 50 nm wide by ~ 90 nm long, while the largest terrace imaged was an oblong surface ~ 250 nm long by ~ 200 nm wide.

The quality of the samples evaporated in our laboratory, both those made using HOPG and mica substrates with and without an adhesion layer of chromium, was greatly improved by hydrogen flame annealing. The STM images of samples that had not been annealed typically showed a large number of amorphous globular surface grains with dimensions of ~ 50 nm. After annealing for ~ 5 minutes in a hydrogen flame, the surfaces appeared polycrystalline with flat terraces with dimensions ranging 70–100 nm. Although annealing clearly improved the appearance of the samples by STM, this step did produce some surface roughness that was visible under a light microscope while the STM tip was being positioned. The source of this roughening is not known, however it is probable that it is a result of the release of adsorbed water from the hygroscopic mica substrate which may have occurred during heating.

Atomic resolution STM images were obtained for both the annealed commercial samples and the annealed laboratory-prepared samples. The gold atoms were arranged in a hexagonal lattice with a spacing measured as 2.85 ± 0.07 Å by STM. The face-centered cubic crystal structure of gold is well known, and such a structure results in a hexagonal lattice of atoms with a spacing of 2.88 Å on the Au(111) surface that is consistent with the structure observed by STM. The Au(111) surface is known to undergo a minor reconstruction which results in a vertical undulation of the surface of 15 pm.[36] Evidence of this reconstruction was not apparent in our STM images.

The addition of a layer of chromium between the substrate material and the gold layer did not appear to improve the adhesion of the gold onto the surface or to result in more durable gold surfaces. The surfaces were easily scratched and damaged both when chromium was used and when it was not. Thus, the presence of a chromium layer did not offer any benefit to the final sample quality. The evaporated gold layer was completely removed from the mica substrate on several occasions after imaging as it would frequently stick to the surface of the clip which was used as an electrical contact.

4.3.4 Conclusions

The laboratory-prepared samples were determined to be of sufficient quality for use as substrates for physisorbed monolayers (see the following section). Although the commercially obtained samples were found to be superior in quality, the improved quality did not offset the added expense associated with these samples. The direct evaporation of gold onto freshly cleaved mica substrates, followed by hydrogen flame annealing, provided both the least expensive and most convenient method of sample preparation, while producing samples of sufficient quality for the observation of physisorbed monolayers. This method allowed the parallel production of multiple gold surfaces and thus eliminated the need to clean and reuse samples; it was thus highly superior to the other surface preparation methods in laboratory practicality.

4.4 Physisorbed Monolayers on Gold

4.4.1 Experimental Details

Saturated solutions of 1-tetradecanol (Acros, 99+%) in tetradecane (Acros, 99%), and 1,14-tetradecanediol (Aldrich, unspecified purity) in dodecane (Acros, ≥ 99%), were prepared and filtered prior to use. A freshly annealed laboratory-prepared sample of gold on mica was placed onto a small piece of copper foil after the sample had been allowed to cool for ~ 30 minutes. The corners of the copper foil were folded over the edge of the sample to allow electrical contact to the gold surface from the back of the sample and the sample and foil were secured in a cell designed to hold liquids during STM imaging. The gold sample was extremely delicate and was easily damaged by mechanical contact. A mechanically cut Pt/Ir 80:20 tip was positioned close to the surface of the sample and then 40 μL of liquid was added to the cell. STM imaging was accomplished using the Nanoscope III STM, as described in Section 4.3.1. Removal of the gold sample from the liquid cell almost invariably destroyed the sample as the gold film would stick to the o-ring that had been pressed against it in order to hold the liquid in the cell.

4.4.2 Results

STM images of physisorbed monolayers on gold surfaces were obtained for both 1-tetradecanol and 1,14-tetradecanediol. Representative STM images of the monolayers are shown in Figures 4.4 and 4.5. The monolayer of 1-tetradecanol was composed of molecules arranged in a herringbone pattern, similar to the structure of monolayers of primary alcohols on HOPG. The observed monolayer structure was consistent with that previously reported by Zhang et al.[23] Molecules in neighboring lamellae are arranged to allow optimal hydrogen bonding to occur between their hydroxyl groups. This orientation results in the measured 124.3 ± 2.3° vertex angle and the V-shape of the herringbone pattern. The orientation of the molecules in the 1-tetradecanol monolayer is indicated in Figure 4.4.

STM images of 1,14-tetradecanediol had not been published prior to this work. The monolayer structure imaged using STM and shown in Figure 4.5 is similar to that seen for terminal diols on HOPG. The molecules are arranged in a herringbone pattern with a 123.8 ± 4.6° vertex at each end where hydrogen bonding occurs. This orientation permits optimal hydrogen bonding at both ends of the molecule. Figure 4.5b shows a larger region of the gold surface. The patch of surface that is covered by the monolayer of 1,14-tetradecanediol is relatively small and has a width of only ~ 20 nm.

4.4.3 Discussion

The successful imaging of physisorbed monolayers by STM on gold surfaces was an important step toward the ultimate goal of this project, the use of physisorbed monolayers as masks for surface patterning. Prior to successfully imaging physisorbed monolayers on these laboratory-prepared gold surfaces, the size of the flat surface terraces that would be sufficient for the formation of stable physisorbed monolayers was not known. Since we were able to image physisorbed monolayers on our laboratory-prepared gold surfaces, it is clear that these surfaces meet the minimum terrace size requirements for the formation of stable physisorbed monolayers. The formation of a stable monolayer of 1,14-tetradecanediol required a terrace width of no more than 20 nm, as can be seen in Figure 4.5b. Of course, the terrace size requirement can be expected to vary with the particular molecules in solution. For example, longer molecules without hydrogen bonding groups may require larger available terrace areas for monolayer formation. Several unsuccessful attempts at imaging long-chain normal alkanes were made in our laboratory and insufficient terrace size on our gold samples is one possible explanation for this failure.

The solvents used in the successful imaging of these physisorbed monolayers on gold surfaces were the normal alkanes tetradecane and dodecane. These solvents were selected following literature examples.[20–23] These solvents are interesting selections because unlike 1-phenyloctane which is commonly used in the study of physisorbed monolayers on HOPG, these normal alkanes are capable of forming their own physisorbed monolayer and thus may compete with the formation of monolayers by the solute. Several attempts were made at imaging physisorbed monolayers at the interface of gold surfaces and phenyloctane-based solutions in our laboratory, but these attempts were not successful. This is an intriguing observation which invites further investigation into the role of the solvent during the formation of physisorbed monolayers onto gold surfaces.

4.4.4 Conclusions

Physisorbed monolayers of 1-tetradecanol and of 1,14-tetradecanediol on laboratory-prepared gold surfaces were imaged using STM. The molecules were oriented in herringbone patterns on the gold surfaces in manners similar to those typically seen for primary alcohols and for terminal diols on HOPG. Stable monolayers formed on terraces as small as 20 nm in width, and it was thus demonstrated that the laboratory-prepared gold samples were of sufficient quality for the formation of stable physisorbed monolayers.

4.5 Physisorbed Monolayers for Masks

4.5.1 Experimental Details

1,3,5-Benzenetricarboxylic acid, or trimesic acid (TMA), and fullerene C_{60} were selected as promising candidates for the formation of physisorbed monolayers that might be used as masks for surface patterning, because monolayers of these molecules incorporate uncovered surface regions into their structure. Since we had not previously imaged monolayers of these molecules in our laboratory, and because the preparation and handling of HOPG substrates is much simpler than that of the evaporated gold samples, STM imaging was performed using HOPG. After successful imaging on HOPG, we proceeded to attempt STM imaging using the laboratory-prepared samples of gold on mica. Grade SPI-1 HOPG was obtained from Structure Probe, Inc., and a fresh surface was obtained by removing a layer with tape before imaging. Gold samples on mica substrates were prepared in the laboratory and annealed as described in Section 4.3.1. Saturated solutions of 1,3,5-benzenetricarboxylic acid (Alfa Aesar, 98%) were prepared in three different solvents: butyric acid (Acros, 99+%); hexanoic acid (Acros, 99+%); and nonanoic acid (Acros, 98+%). The HOPG sample was clamped into a cell that is designed to contain liquids while permitting STM imaging. Gold samples were clamped into the identical cell after a piece of copper or gold foil had been placed between the bottom of the cell and the sample and the corners of the foil folded over the sample edge to allow electrical contact to the gold film. A mechanically cut Pt/Ir 80:20 tip was positioned above the sample surface and 40 μL of solution were added to the cell. Samples were then imaged using the Nanoscope III STM system previously described.

Fullerene C_{60} (> 99%) was obtained from TCI America, Inc., and dissolved in benzene. Fullerene films were prepared on the HOPG substrates by submersing the HOPG in a petri dish containing pure water. Several drops of fullerene solution were added to the dish and it could be seen that the contents of these drops spread across the surface of the water. The HOPG sample was then held at an angle of about 60° to the surface of the water and slowly removed from the dish and dried in a stream of nitrogen. Fullerene films were prepared on the gold surfaces using a similar technique, however it was essential for the gold substrates to be sealed into the STM liquid cell before placement into the petri dish. Exposure of the mica substrate to water or water-containing liquids resulted in the rapid removal of the gold film. The dried samples were then imaged using the Nanoscope III STM as previously detailed.

4.5.2 Results

Physisorbed monolayers of TMA on HOPG were successfully imaged using STM. Representative STM images of these monolayers are shown in Figure 4.6. The formation of hydrogen bonds is primarily responsible for the formation of ordered monolayers of TMA. There are multiple ways in which the hydrogen bonding can occur, and models of three potential monolayer structures are shown in Figure 4.7. The structure of the monolayer was found to be dependent upon the solvent used, which was consistent with previously published reports.[37] When butyric acid was used as solvent, the structure modeled in Figure 4.7b was observed; however when nonanoic acid was used as solvent, the structure modeled in Figure 4.7a was observed. We did not observe the third structure, that shown in Figure 4.7c in monolayers on HOPG. For both solvents it was observed that the TMA monolayers were only stable when the HOPG was held under negative bias. If the sample bias was changed to a positive value, the monolayer could be imaged for a time but would disappear within several minutes.

TMA monolayers were also successfully imaged on the laboratory-prepared gold samples. STM images of TMA monolayers on gold are shown in Figure 4.8. These monolayers were prepared using hexanoic acid as solvent, and the structure observed was a simple hexagonal arrangement of molecules with a spacing measured to be 8 Å. This structure most resembled that modeled in Figure 4.7c. Although fresh monolayers were imaged clearly on several occasions, the monolayer structure was observed to disappear after ~ 40 minutes of imaging. This phenomenon was observed on multiple occasions and thus it seems more likely that a change in surface structure was occurring than that the tunneling tips were reproducibly losing their ability to resolve molecules on the gold surface.

An STM image of a layer of fullerene C_{60} on HOPG is shown in Figure 4.9. The molecules were arranged in a hexagonal pattern on the surface with a spacing of 15 Å. It is believed that the image is of a monolayer of fullerene, but it is possible that more than one layer is present. An ordered fullerene layer was not observed on the gold surface. An STM image of the resulting film is shown in Figure 4.10. Fullerene molecules appeared to cover the gold surface in a disordered manner and possibly in multiple layers.

4.5.3 Discussion

TMA and fullerene appear to be promising candidates for molecules that will form physisorbed monolayers that can be used as masks for surface patterning using the approach outlined in Section 4.2. Monolayers of TMA were successfully imaged both on HOPG and gold substrates. A fullerene layer was successfully imaged on HOPG, but the layer observed on the gold surface was disordered. However, additional challenges were encountered as described below.

The monolayers of TMA which formed on the gold surfaces appeared to be unstable with time, reproducibly disappearing after ~ 40 minutes of imaging with the STM. The cause of this instability is unknown, but is likely to be the relatively high acidity of the molecule ($pK_1 = 2.1$, $pK_2 = 4.1$, $pK_3 = 5.18$).[25] The carboxylic acids used as solvents appeared to be a curious choice due to their ability to competitively form a monolayer of their own, however we did not observe any monolayers of TMA using other solvents such as 1-phenyloctane. The solvent-dependent monolayer structures appear to indicate a role for the solvent in the formation of TMA monolayers. Solvent acidity may be important in the prevention of the loss of H^+ from the carboxylic acid groups which may then interfere with the formation of the hydrogen-bonded monolayer network.

Other researchers have observed potential-dependent structures of TMA monolayers on gold surfaces in aqueous acids.[24,25] The monolayer structures were altered as protons were removed from the acid groups of the TMA molecules. Several different surface structures were observed, many of which incorporated carboxylate groups which were coordinated with the underlying gold surface. Such coordination resulted in the TMA molecules standing on the surface rather than lying flat. It thus seems likely that loss of H^+ from the acid groups on the TMA molecules produces disorder in the monolayers on gold surfaces and is responsible for their observed instability. The observation that the structure of the TMA monolayer on HOPG surfaces required that the sample be held under negative bias also suggests that changes in the acid groups of TMA may play a role in the apparent instability of the monolayers. Thus in order to proceed with the development of a surface patterning technique based upon the use of physisorbed TMA monolayer masks, the development of the ability to image surfaces with STM under conditions where the sample potential and the concentration of H^+ in the solution are both controlled and well defined would be highly useful for our laboratory.

Although a fullerene layer was successfully imaged on an HOPG substrate, the film imaged on the gold surface was very disordered and would not be useful as a mask for surface patterning. Improved fullerene films may be produced using more refined experimental techniques that would permit control over the film deposition parameters. Thus the fullerene film would likely be improved through the use of a commercial Langmuir–Blodgett trough. A method for producing very highly ordered fullerene monolayers on gold surfaces has been reported by Uemura et al.[38] The method involves the electrochemical replacement of an adsorbed iodine layer on the gold surface by fullerene molecules. Implementation of this method would be greatly assisted by the ability to image the gold surface with our STM under conditions where the sample potential is both controlled and well defined.

Both TMA and fullerene C_{60} are known to form physisorbed monolayers on gold surfaces and may be useful as masks for surface patterning. However, control over sample potential during STM imaging would greatly improve the likelihood of successful masking and thus improve the likelihood of successful surface patterning using either of these molecules. Sample potential can be controlled and defined during STM imaging through the use of the well-established technique of electrochemical scanning tunneling microscopy (ECSTM). ECSTM permits STM imaging in liquids that allow the flow of Faradaic current. The sample is incorporated into an electrochemical cell and serves as the working electrode. A counter electrode and a reference electrode are included in the cell to allow full control over the cell potential. The technique requires that the STM tip be fully insulated except for an extremely small (~ 10 nm^2) area at the tip. The insulation is required to limit the flow of Faradaic current at the tip to a value significantly smaller than that of the tunneling current.

The STM tip can be modeled as a hemispherical ultra-microelectrode. The expression for the steady state current at such an electrode is $i_{ss} = 2\pi n F D_O C_O^* r_0$, where n is the stoichiometric number of electrons involved in the electrode reaction, F is the Faraday constant, D_O is the diffusion constant, C_O^* is the bulk concentration for the oxidized species, and r_0 is the radius of the hemisphere. Typical values for these variables lead to $i_{ss} \approx \frac{0.6\mathrm{nA}}{\mu\mathrm{m} \times \mathrm{mM}}$. Thus, the Faradaic current can be reduced to a level where it is significantly smaller than the tunneling current when r_0 is on the order of a few nanometers.

The preparation of tips that meet this requirement and which provide adequate resolution for STM imaging is difficult and is necessarily a low yield process. Several methods have been described; however the experience in our laboratory indicates that the most promising method is that which was described by Heben et al.[39–41] This method involves coating electrochemically etched Pt tips with a polymer melt. A nanometer-scale hole can then be opened in the insulation at the very end of the pointed part of the tip using a field emission process. Although we have recently been able to image surfaces under aqueous acidic solutions using ECSTM techniques and tips prepared in this manner, we have not recently achieved atomic resolution under these demanding conditions. However, this has been accomplished in our laboratory in the past, and therefore it appears likely that these results can again be achieved.

4.5.4 Conclusions

Physisorbed monolayers of TMA have been observed on both HOPG and gold surfaces. A physisorbed layer of fullerene was also observed on HOPG. Spaces are incorporated into the monolayer structures of these molecules and thus such monolayers may be useful as masks for a surface patterning technique. The monolayers of TMA on gold were observed to be unstable over time, and the fullerene film observed on the gold surface was highly disordered. ECSTM may offer remedies to both of these issues and it may prove highly useful to redevelop this ability in our laboratory.

4.6 Summary

Physisorbed monolayers that incorporate spaces into their structure may be useful as masks in a surface patterning technique analogous to photolithography. Gold–thiol chemistry may provide a route toward the formation of chemical bonds to surface areas left uncovered by the physisorbed monolayer mask. Gold surface preparation techniques were evaluated and it was found that evaporation of gold onto mica substrates followed by annealing of the samples in a hydrogen flame for ~ 5 minutes produced polycrystalline gold samples with Au(111) surfaces. Physisorbed monolayers of 1-tetradecanol, 1,14-tetradecanediol were observed on the gold surfaces. Monolayers of 1,3,5-benzenetricarboxylic acid (TMA) were observed on both HOPG and gold surfaces. The stability of the TMA monolayers appeared to depend upon the sample bias. It is believed that the acidity of the TMA molecule may be the cause of the observed instability over time of its monolayers on gold surfaces. An ordered layer of fullerene C_{60} was observed on HOPG but not on a gold surface. Both TMA and fullerene are promising candidates for masking layers for use in a nanometer scale chemical surface patterning technique; however the formation of stable, ordered monolayers of these molecules appears to require that our laboratory redevelop the ability to perform STM imaging in electrochemical environments. The development of such capability will certainly require patience and commitment as the preparation of tips suitable for STM imaging under an electrochemical environment is a low-yield process. However, the additional experimental capabilities gained by redeveloping this technique in our laboratory will likely justify such efforts.

Figure 4.1 STM Image of a Large Monolayer Domain

A constant-current STM image of di-*n*-octadecylsulfide on HOPG. Several domains are visible in the image and the domain boundaries have been marked with dashed white lines. One very large monolayer domain covers almost the entire imaging area. The domain is at least 217 nm wide by 300 nm long and presumably extends beyond the area of the image. Imaging conditions were 1200 mV bias, 200 pA current, and a scan rate of 10.2 Hz.

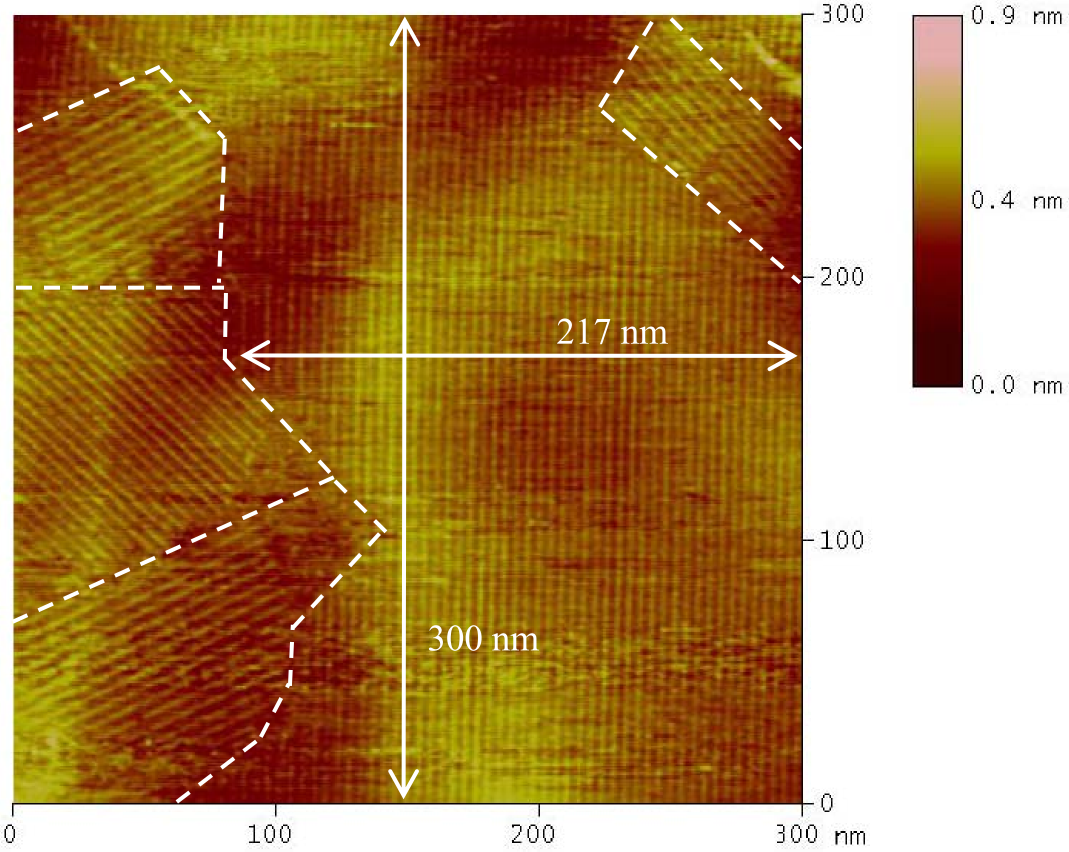

Figure 4.2 STM Images of Evaporated Gold Surfaces

(a) A constant current image of HOPG for comparison purposes. Imaging conditions were sample bias = 100mV, current = 2 nA, scan rate = 15.3 Hz.

(b) A freshly etched, hydrogen terminated, n-type Si(111) surface also for comparison purposes. Imaging conditions: -3000 mV, 75 pA, 10.2 Hz

(c) Gold evaporated directly onto HOPG. Imaging conditions: 100 mV, 1 nA, 10.2 Hz

(d) The sample from (c) after annealing in a hydrogen flame for ~ 5 minutes. Imaging conditions: 310 mV, 500 pA, 10.2 Hz

(e) Gold evaporated on chromium on HOPG. Imaging conditions: 300 mV, 2 nA, 10.2 Hz.

(f) The sample shown in (e) after annealing for ~ 5 minutes. Imaging conditions: 200 mV, 2 nA, 15.3 Hz

(g) Gold evaporated directly onto mica. Imaging conditions: 150 mV, 2 nA, 10.2 Hz

(h) The sample shown in (g) after annealing for ~ 5 minutes under identical imaging conditions

(i) Gold evaporated on chromium on mica. Imaging conditions: 150 mV, 2 nA, 10.2 Hz

(j) The sample shown in (i) after annealing for ~ 5 minutes under identical imaging conditions

(k) Purchased sample of gold on mica. Imaging conditions: 310 mV, 500 pA, 10.2 Hz

(l) The sample shown in (k) under identical imaging conditions after annealing for ~ 1 minute

Figure 4.2 STM Images of Evaporated Gold Surfaces

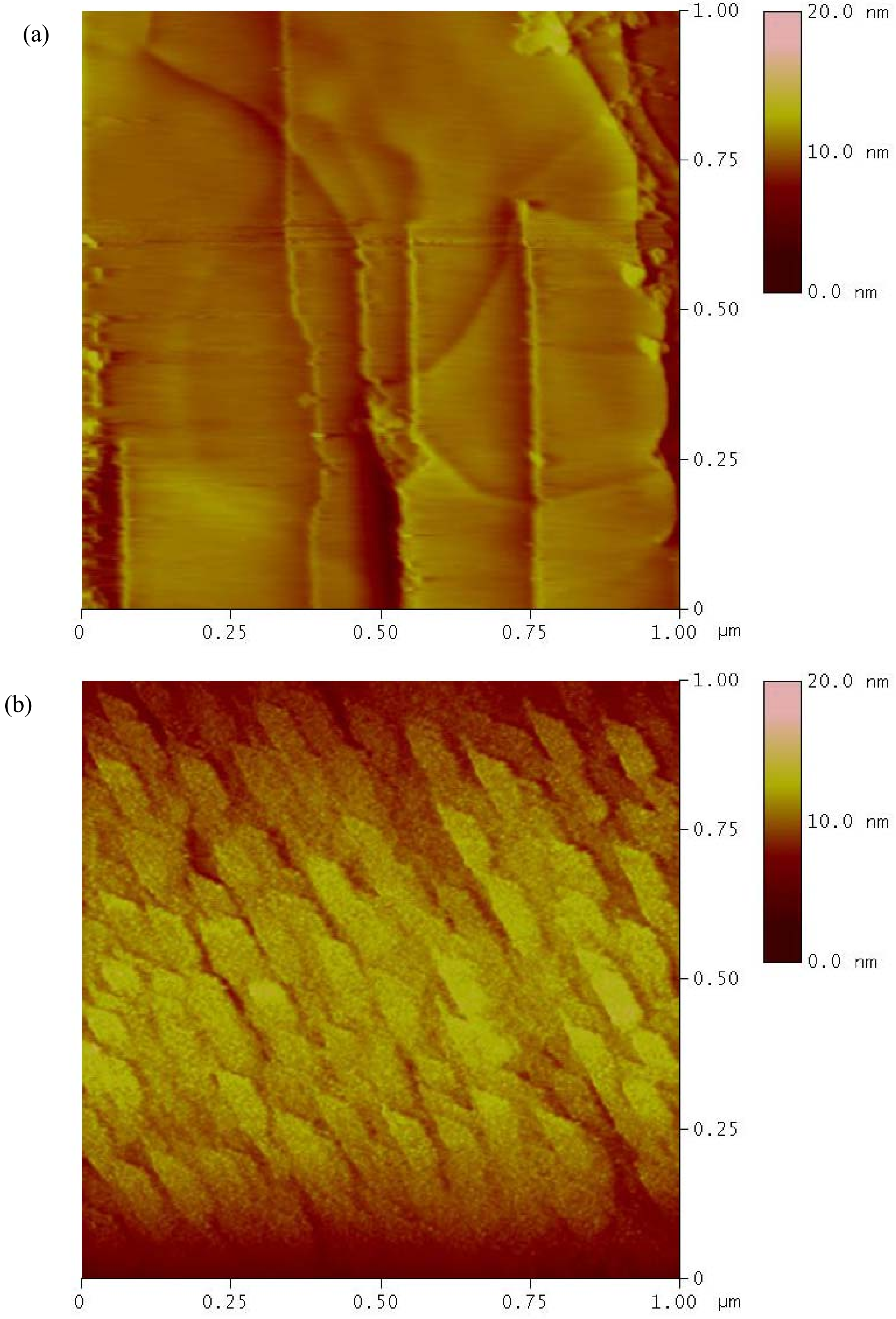

Figure 4.2 STM Images of Evaporated Gold Surfaces

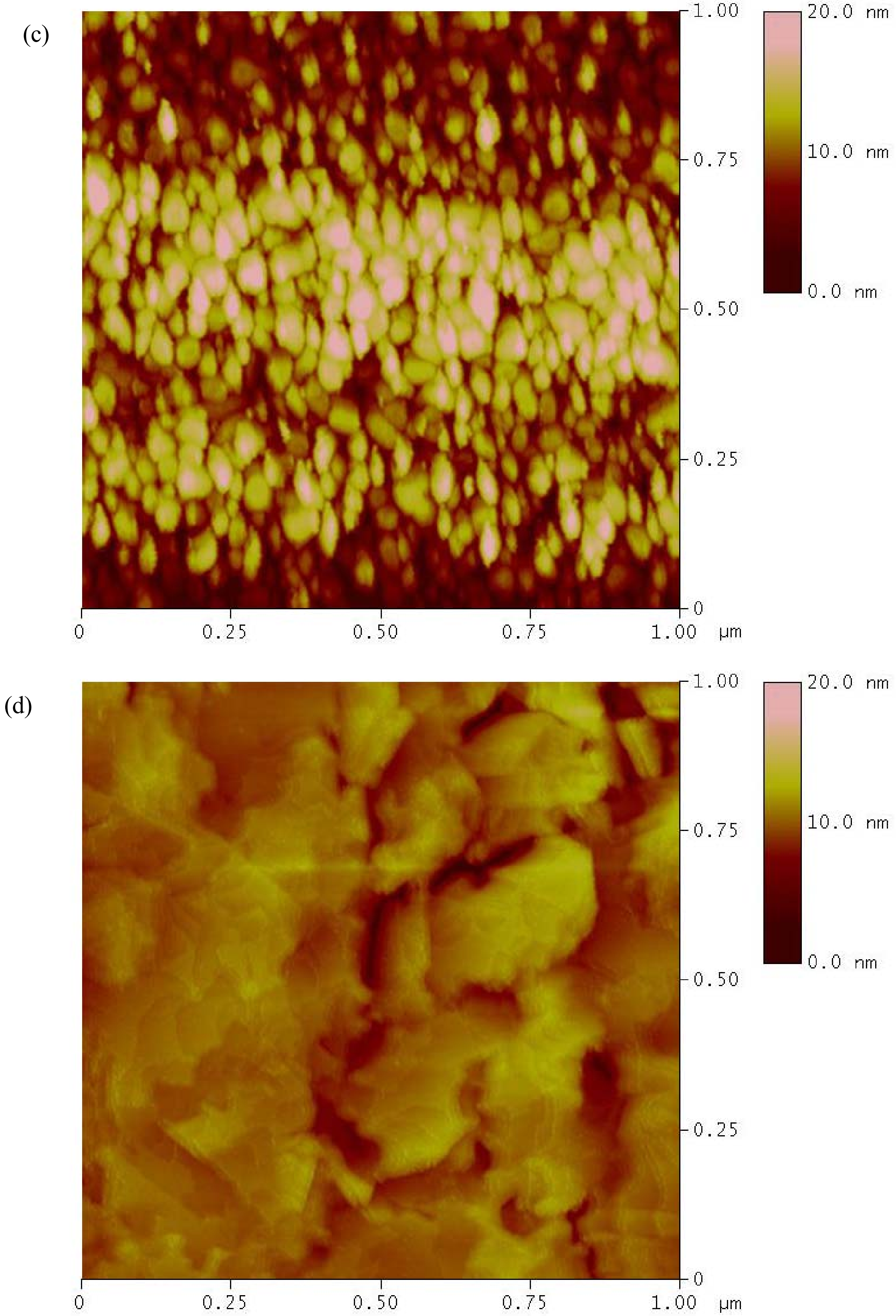

Figure 4.2 STM Images of Evaporated Gold Surfaces

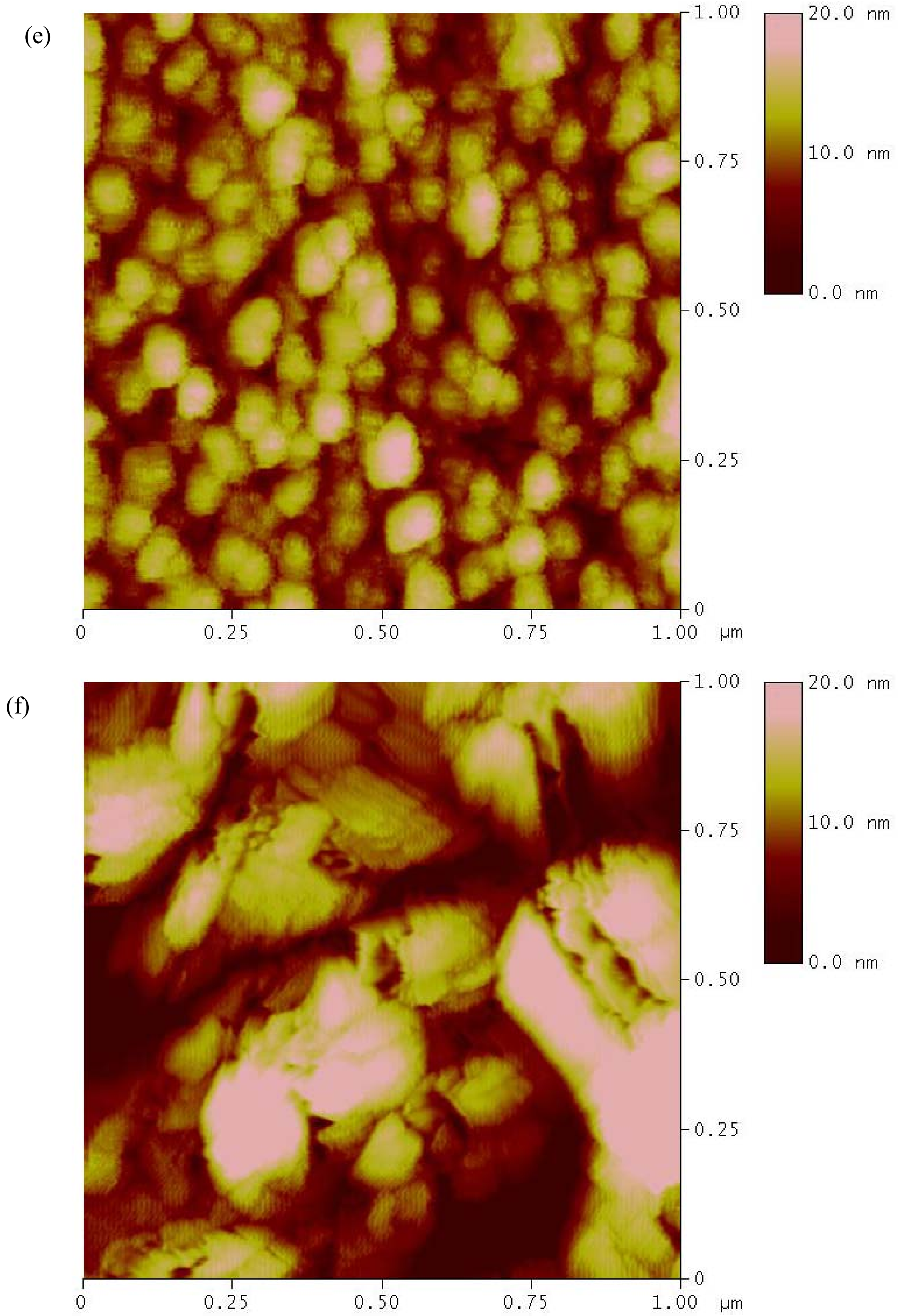

Figure 4.2 STM Images of Evaporated Gold Surfaces

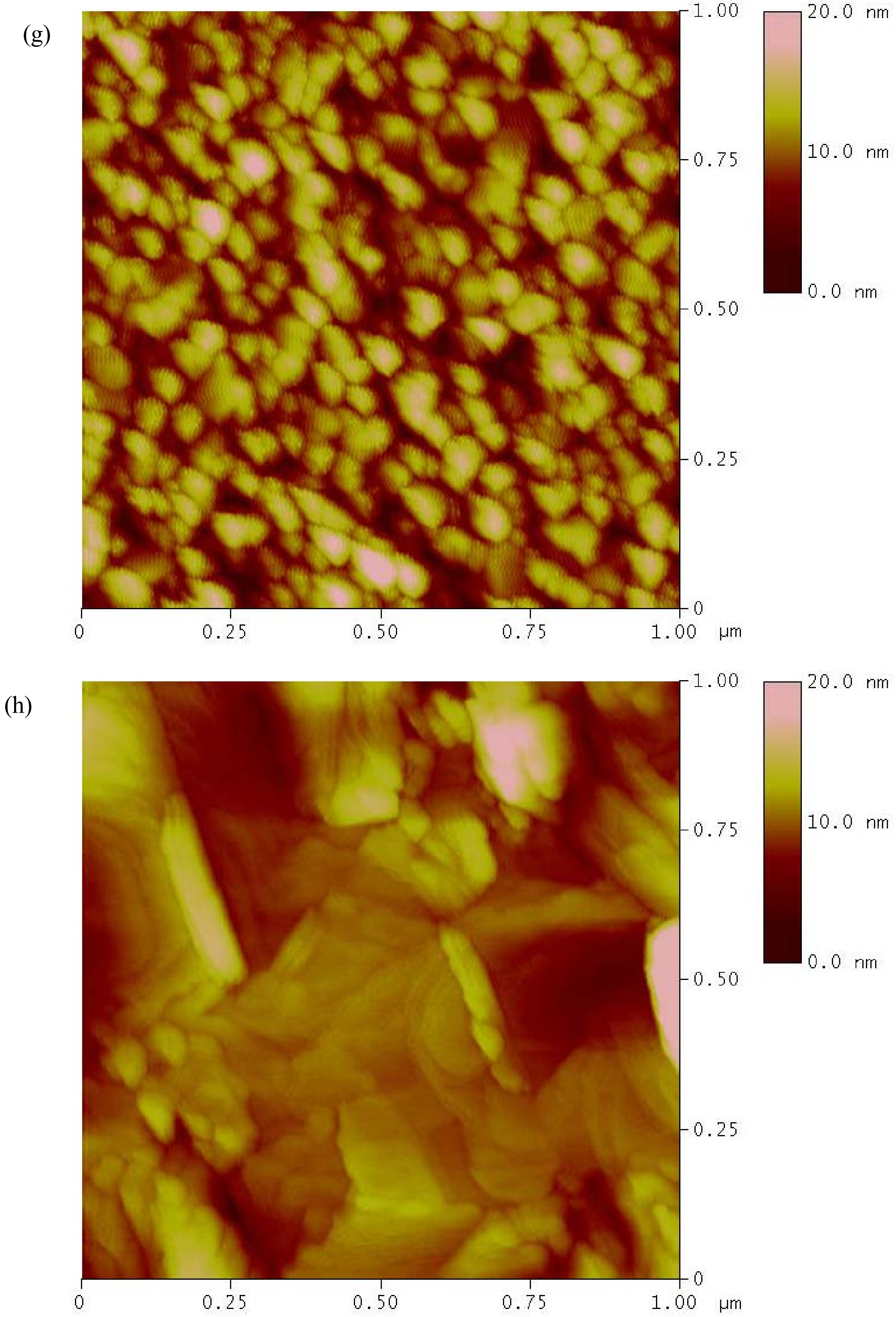

Figure 4.2 STM Images of Evaporated Gold Surfaces

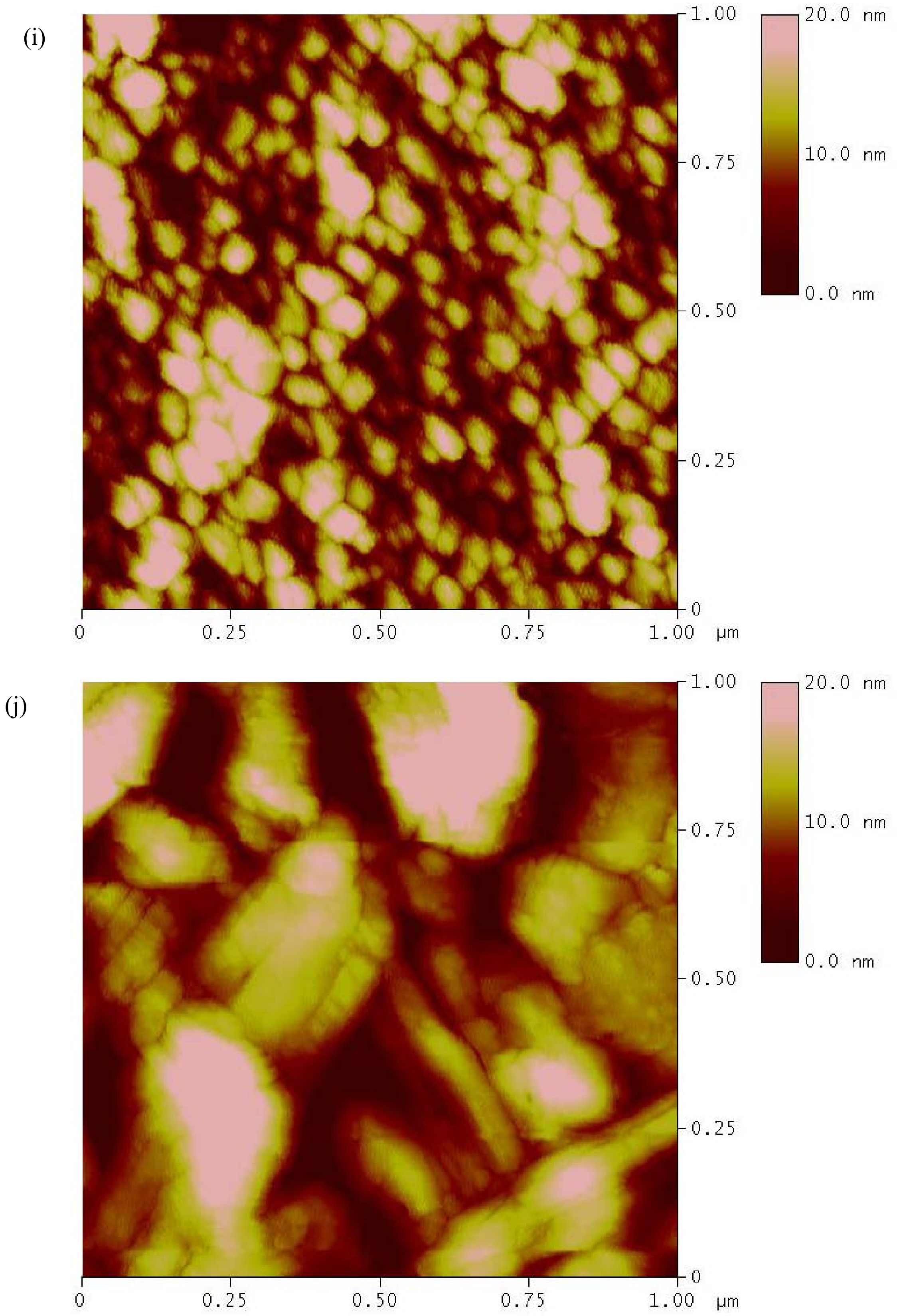

Figure 4.2 STM Images of Evaporated Gold Surfaces

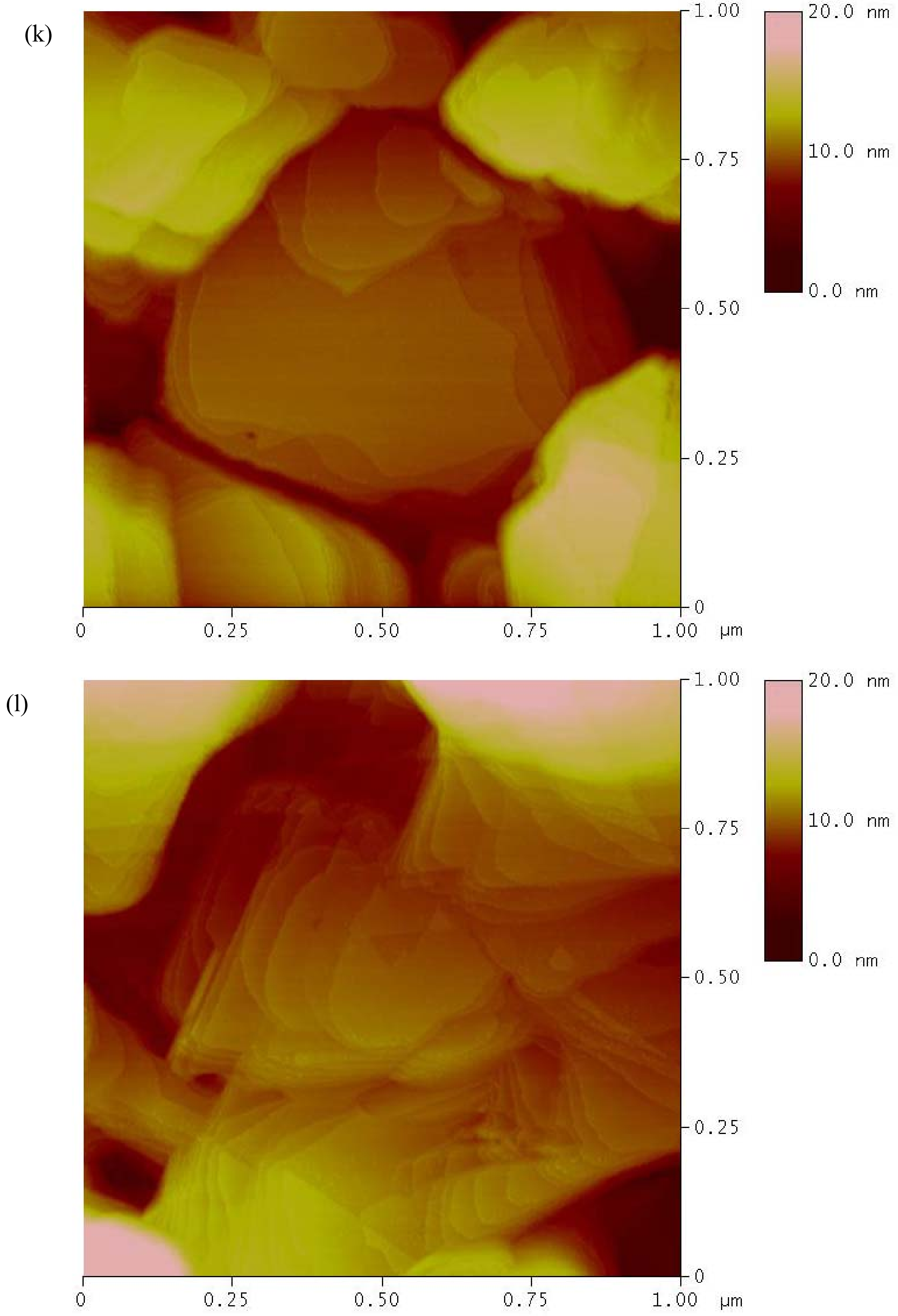

Figure 4.3 Atomic Resolution Images of Gold Samples

(a) STM image of a commercially prepared sample of gold on mica. The distance between atoms in the hexagonal array on the surface was measured to be 2.9 Å. The known spacing of atoms on the Au(111) surface is 2.88 Å. Imaging conditions were 4.795 mV bias, 2 nA, 20.3 Hz.

(b) An image of a laboratory-prepared sample of gold evaporated onto a mica substrate. Atoms are resolved in the image and the distance measured for their spacing on the surface is 2.8 Å. Effects of thermal drift are apparent in the image and produce the apparent compression in one dimension. Imaging conditions were 5 mV bias, 2 nA, and 30.5 Hz.

Figure 4.3 Atomic Resolution Images of Gold Samples

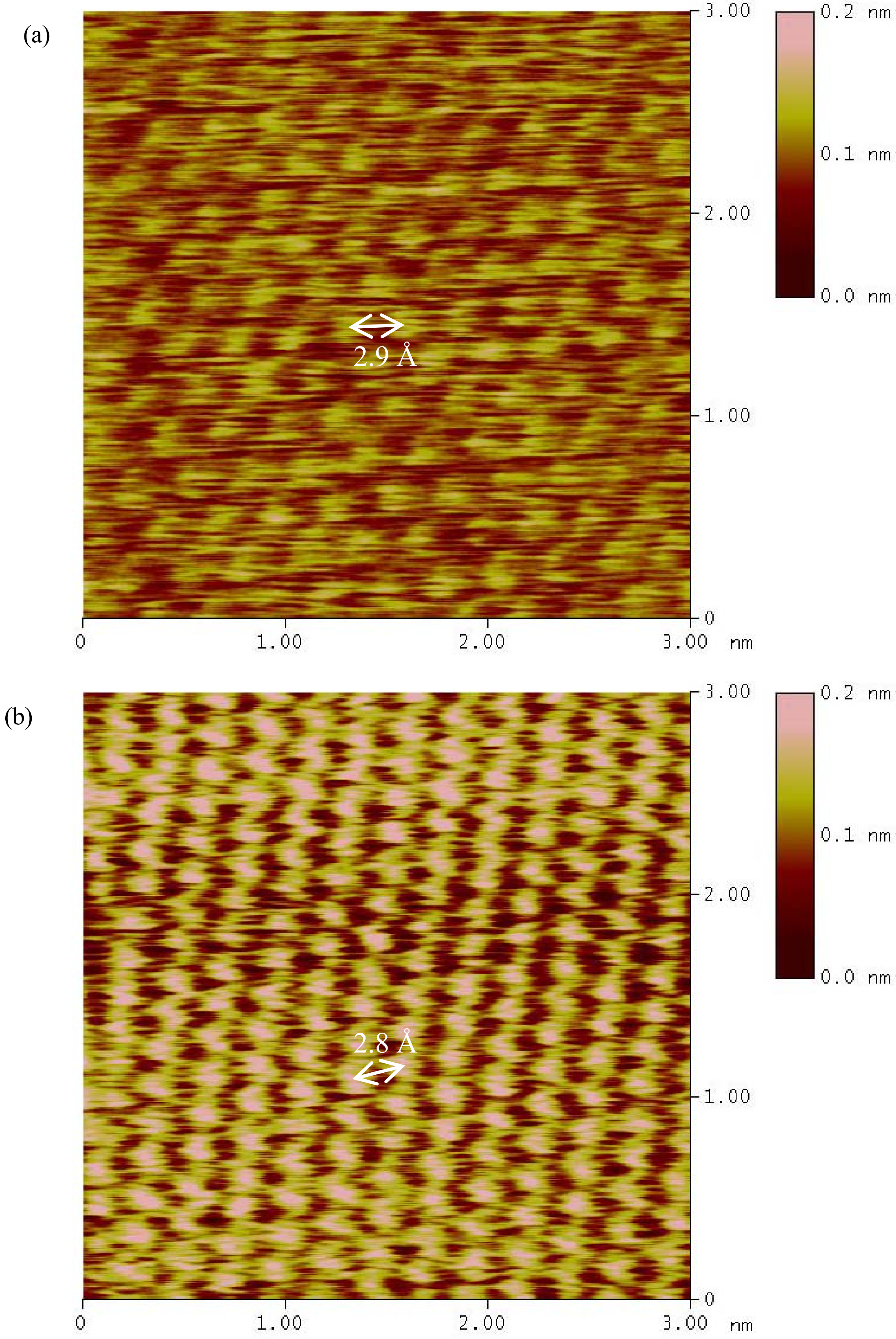

Figure 4.4 STM Image of 1-Tetradecanol on Gold

A constant-current STM image of a monolayer of 1-tetradecanol formed at the liquid–solid interface of a saturated solution of 1-tetradecanol in tetradecane and gold. The molecules are arranged in a herringbone pattern, similar to that observed for physisorbed alcohols on HOPG. The positions of several molecules are marked by white lines. A domain boundary is visible on the right side of the image. Imaging conditions were 35 mV sample bias, 475 pA, and 30.5 Hz.

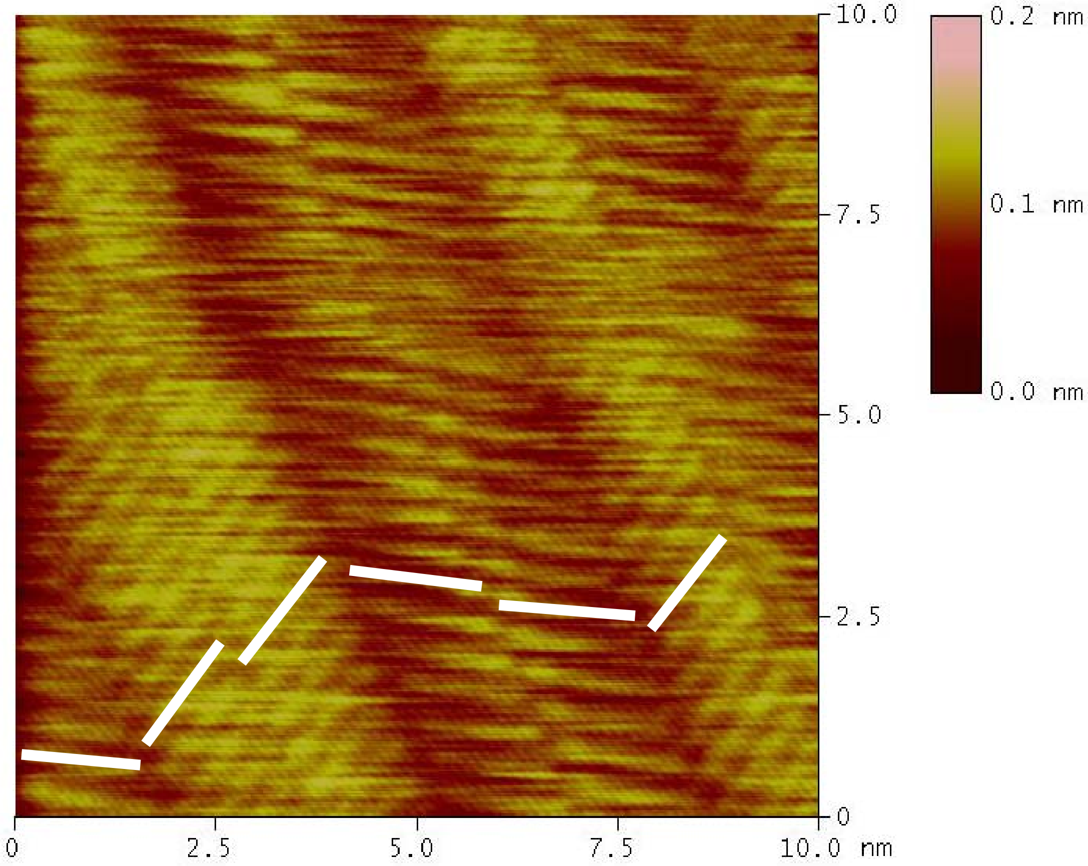

Figure 4.5 STM Images of 1,14-Tetradecanediol on Gold

(a) A constant current STM image of a monolayer of 1,14-tetradecanediol on gold. A herringbone pattern, typical of that seen on HOPG is clearly resolved. A domain boundary is indicated by the dashed white line. The imaging conditions were 35 mV bias, 475 pA, and 30.5 Hz.

(b) The monolayer shown in (a) showing a larger area of the surface. The monolayer covers a relatively small area of the surface, and is only ~ 20 nm in width. The imaging conditions were identical to those for (a).

Figure 4.5 STM Images of 1,14-Tetradecanediol on Gold

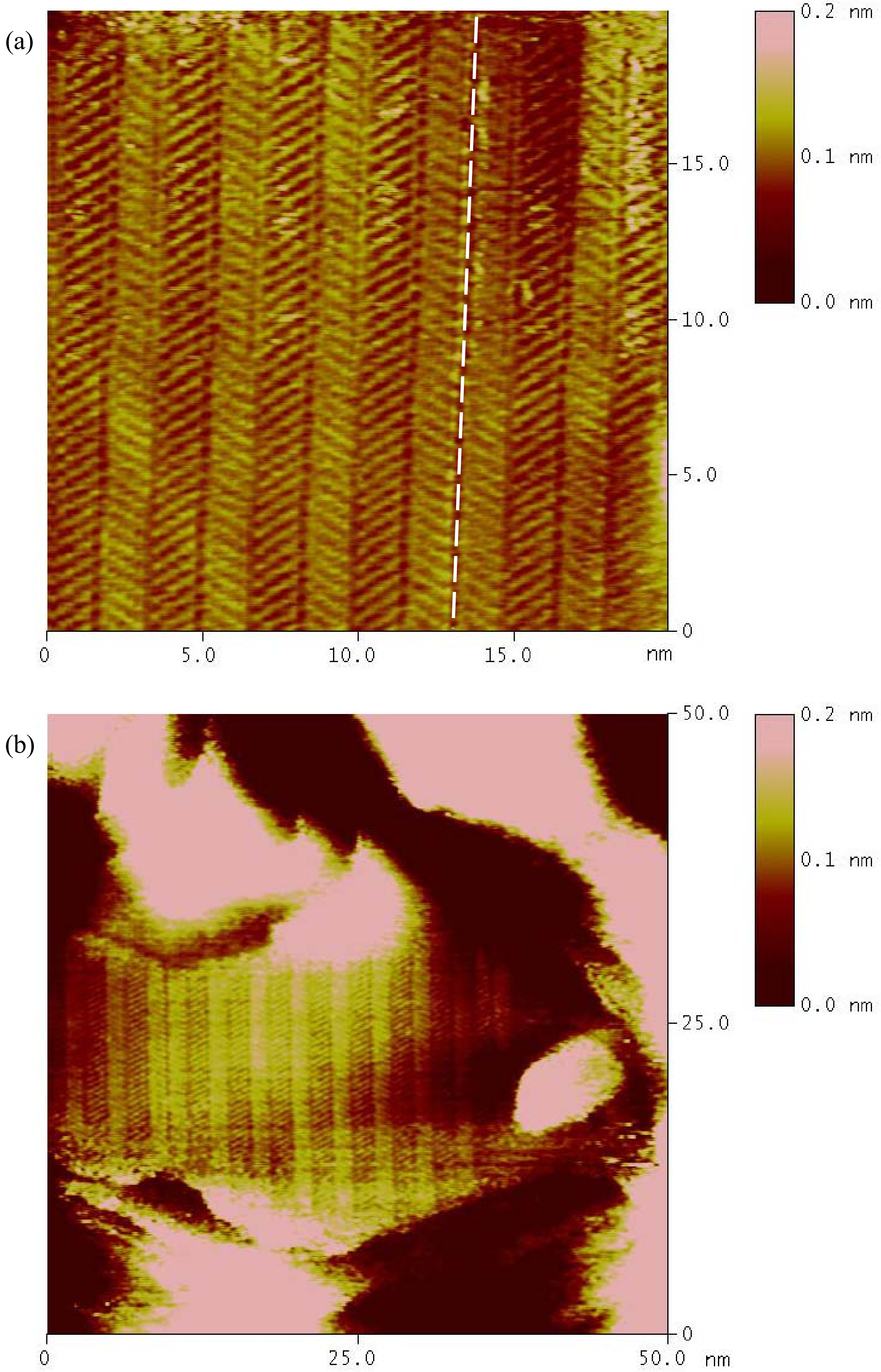

Figure 4.6 STM Images of 1,3,5-Benzenetricarboxylic Acid (TMA) on HOPG

(a) Constant-current STM image of TMA in butyric acid on HOPG. The monolayer exhibits a hexagonal structure with a spacing measured to be 12 Å and a second spacing measured to be 9 Å. This is consistent with the structure modeled in Figure 4.7b. The imaging conditions were -1170 mV sample bias, 150 pA, and 30.5 Hz.

(b) Constant-current STM image of TMA in nonanoic acid on HOPG. The monolayer has a hexagonal structure with a spacing measured to be 17 Å. This is the structure modeled in Figure 4.7a. The image contrast appears to be reversed. The imaging conditions were -1214 mV, 75 pA, and 30.5 Hz.

Figure 4.6 STM Images of 1,3,5-Benzenetricarboxylic Acid (TMA) on HOPG

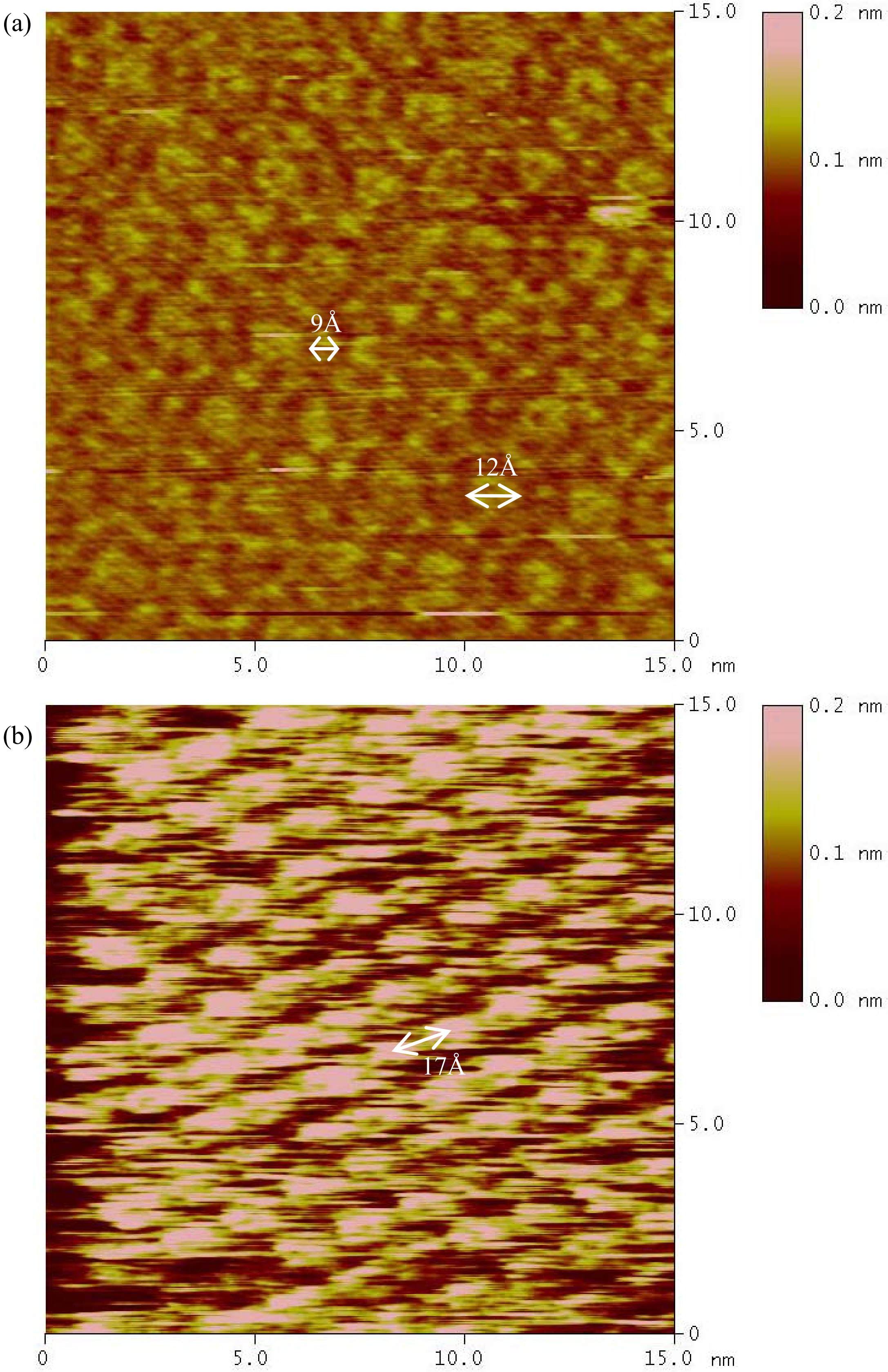

Figure 4.7 Models of TMA Monolayer Structures

Several structures are possible for physisorbed monolayers of TMA. Multiple structures are possible because the carboxylic acid groups can form hydrogen bonds in more than one way.

(a) This structure is known as a “chicken wire” structure. All of the carboxylic acid groups are arranged to hydrogen bond in pairs.

(b) This structure is known as the “flower” structure. Some of the carboxylic acids form hydrogen bonding pairs, while other hydrogen bonding groups contain three acid groups.

(c) This structure is known as the “super flower” structure. In this structure, three carboxylic acid functional groups are involved in each hydrogen bonding group.

Figure 4.7 Models of TMA Monolayer Structures

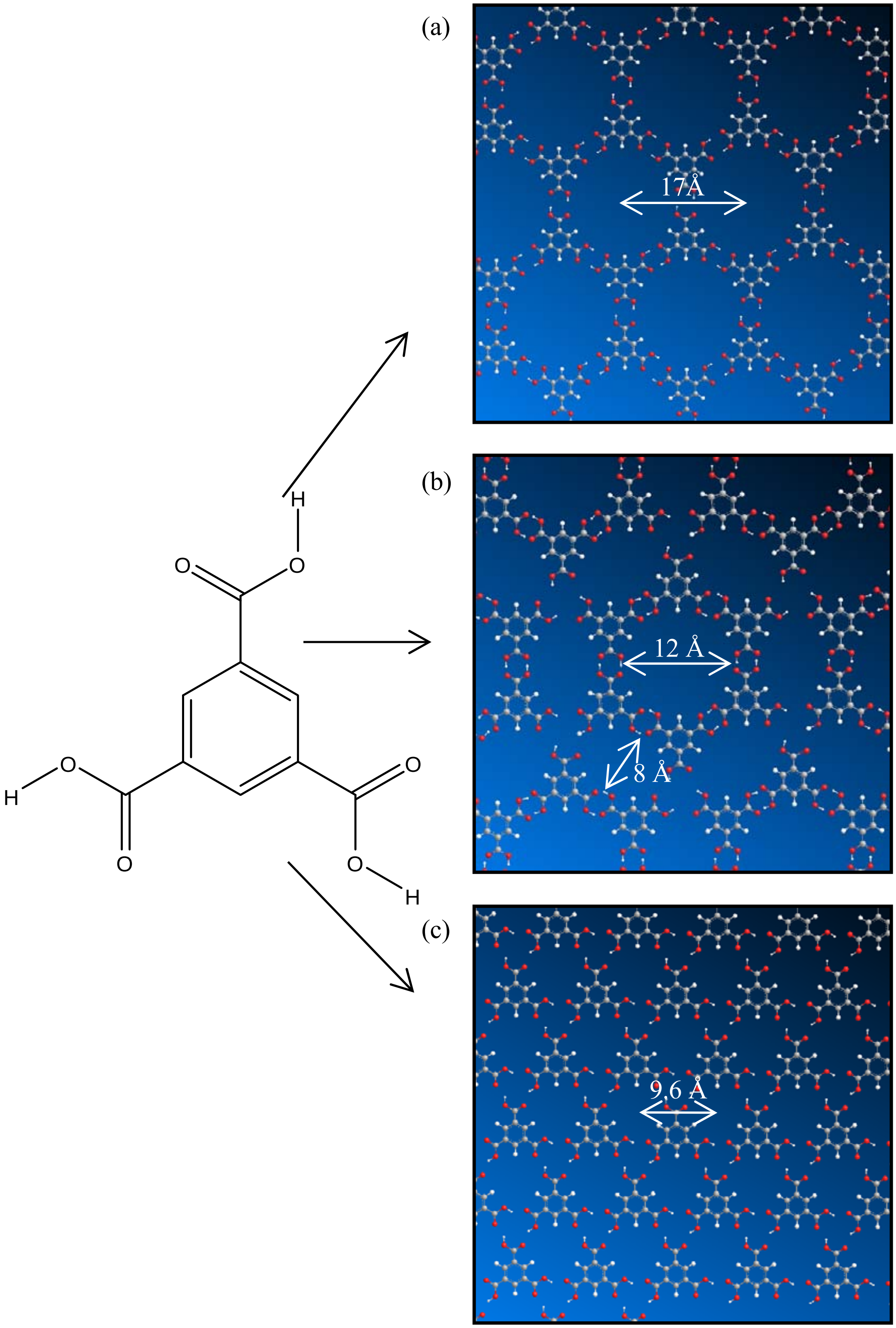

Figure 4.8 STM Images of TMA on Gold

(a) A constant-current STM image of TMA on an evaporated and annealed gold on mica substrate. Hexanoic acid was used as a solvent for the TMA. The monolayer structure consists of a hexagonal arrangement of molecules with a spacing measured as 8 Å. This structure closely resembles the model in Figure 4.7c. Imaging conditions were -75 mV sample bias, 100 pA, and 20.3 Hz.

(b) A larger scale STM image of the sample shown in (a). The arrow indicates a location in the structure where a molecule is missing. Imaging conditions were -300 mV sample bias, 100 pA, and 20.3 Hz.

(c) A larger scale STM image of the sample shown in (a) and (b). The monolayer covers the entire image area and a few flaws are visible in the structure. The imaging conditions were -300 mV sample bias, 100 pA, and 30.5 Hz.

Figure 4.8 STM Images of TMA on Gold

(a)

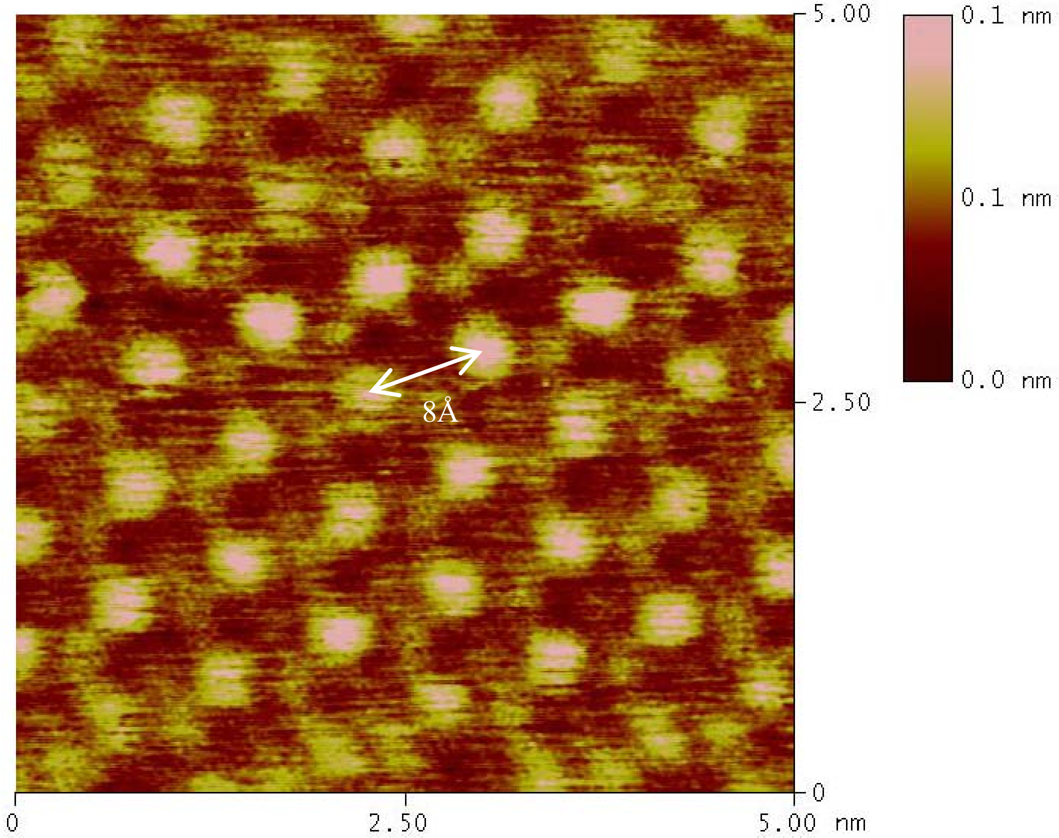

Figure 4.8 STM Images of TMA on Gold

(b)

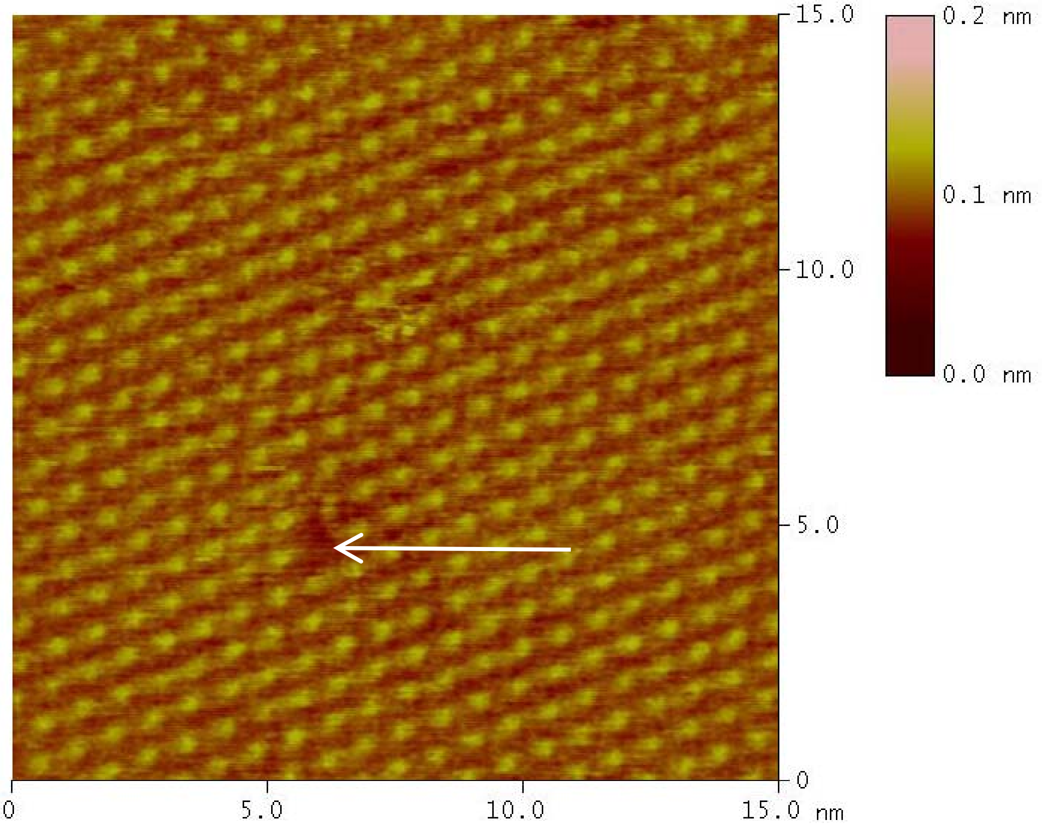

(c)

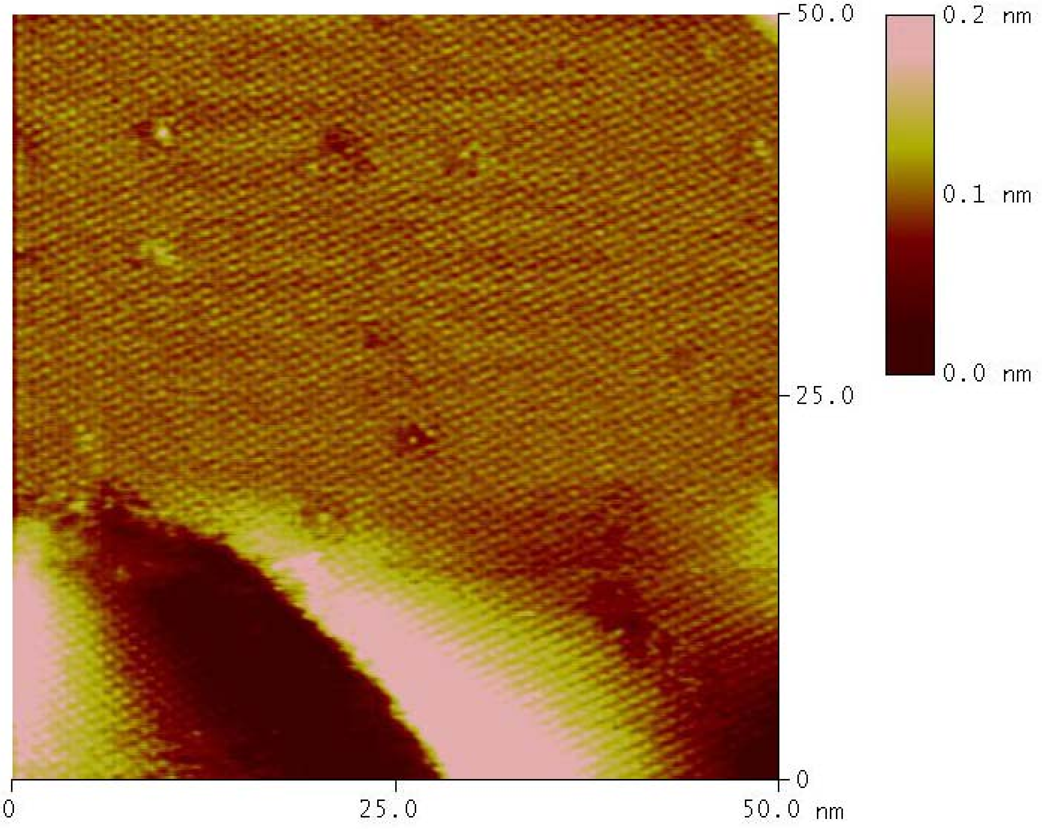

Figure 4.9 STM Image of Fullerene C_{60} on HOPG

A constant-current STM image of fullerene C_{60} on HOPG. The molecules are arranged in a hexagonal pattern on the surface with a measured spacing of 15 Å. The imaging conditions were -1200 mV sample bias, 2 nA, and 30.5 Hz.

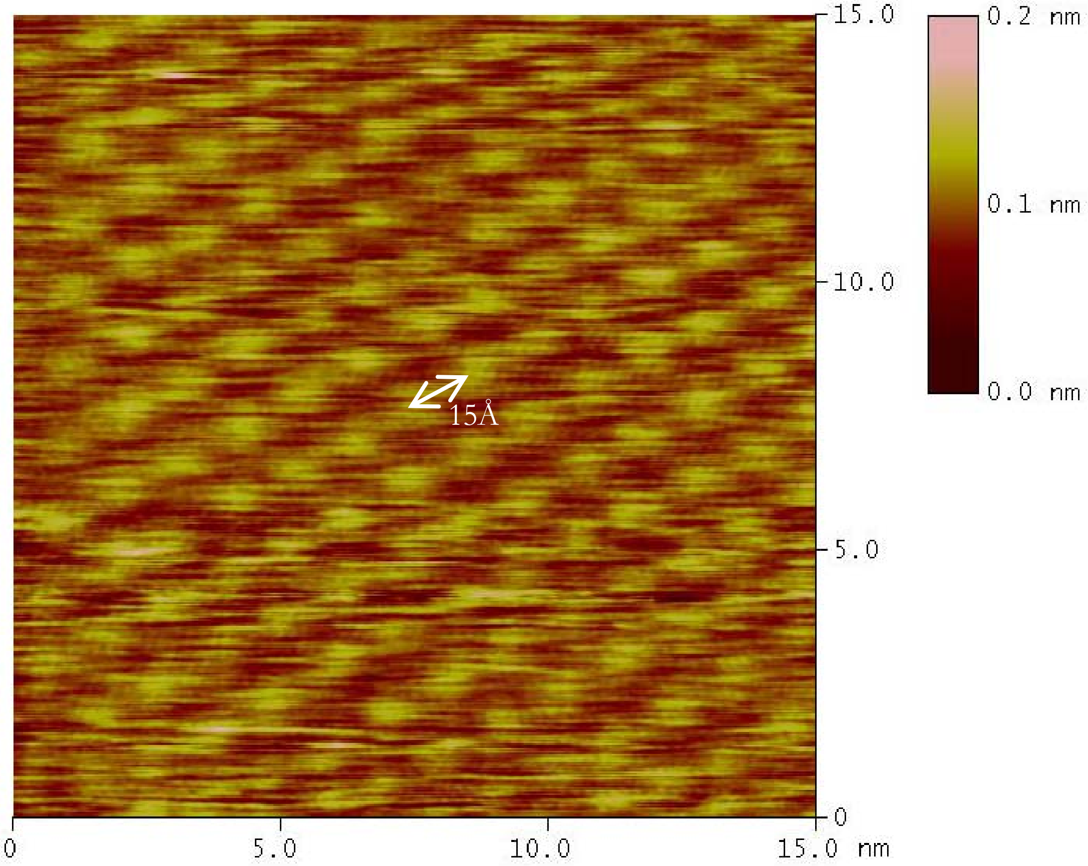

Figure 4.10 STM Image of Fullerene C_{60} on Gold

A constant-current STM image of a film of fullerene on a gold surface. The molecules cover the surface in a disordered manner and possibly in several molecular layers. The imaging conditions were 400 mV, 2 nA, and 30.5 Hz.

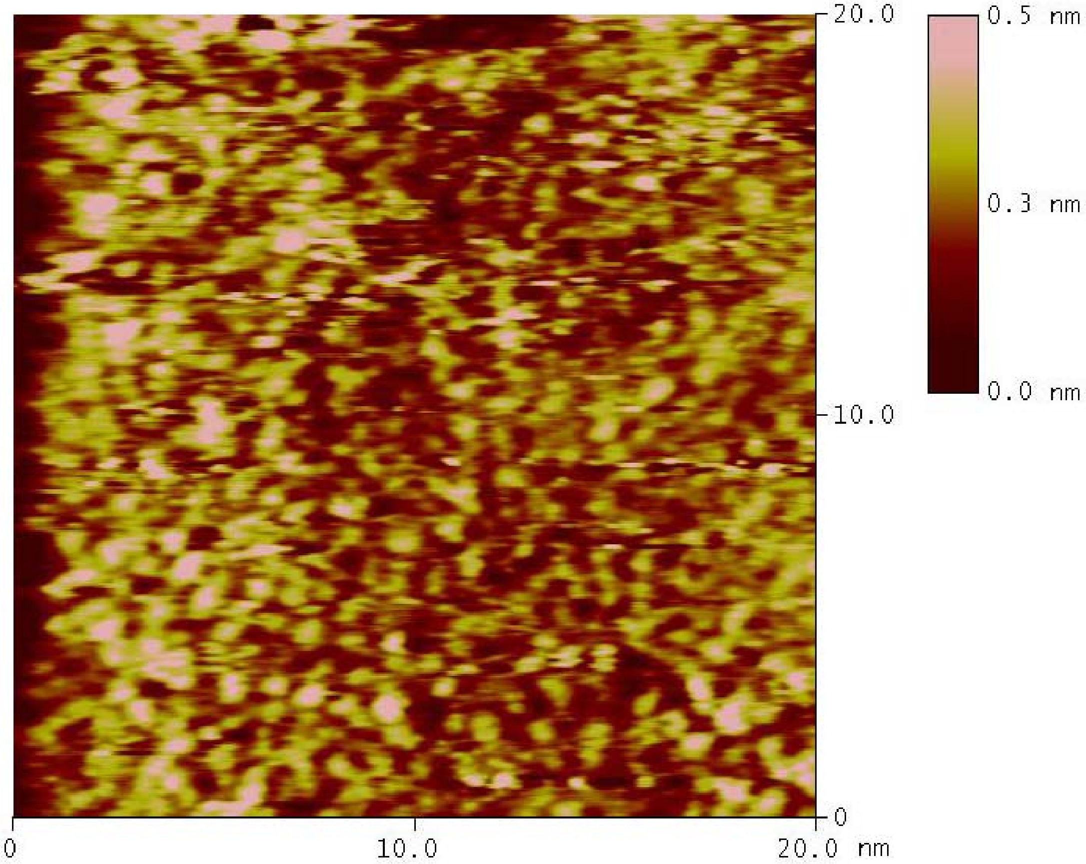

4.7 References

(1) Groszek, A. J. *Nature* **1962,** *196*, 531–533.

(2) Groszek, A. J. *Nature* **1964,** *204*, 680.

(3) Everett, D. H. *Transactions of the Faraday Society* **1965**, *61*, 2478–2495.

(4) Ash, S. G.; Everett, D. H.; Findenegg, G.H. *Transactions of the Faraday Society* **1968**, *64*, 2639–2644.

(5) Hentschke, R.; Winkler, R. G. *J. Chem. Phys*. **1993**, *99*, 5528–5534.

(6) Castro, M. A.; Clarke, S. M.; Inaba, A.; Dong, C. C.; Thomas, R. K. *J. Phys. Chem. B* **1998**, *102*, 777–781.

(7) Findenegg, G. H.; Liphard, M. *Carbon* **1987**, *25*, 119–128.

(8) McGonigal, G. C.; Bernhardt, R. H.; Thomson, D. J. *Appl. Phys. Lett.* **1990,** *57*, 28–30.

(9) Uosaki, K.; Yamada, R. *J. Am. Chem. Soc.* **1999,** *121*, 4090–4091.

(10) Bain, C. D.; Troughton, E. B.; Tao, Y. T.; Evall, J.; Whitesides, G. M.; Nuzzo, R. G. *J. Am. Chem. Soc.* **1989,** *111*, 321–335.

(11) Dishner, M. H.; Ivey, M. M.; Gorer, S.; Hemminger, J. C.; Feher, F. J. *J. Vac. Sci. Technol., A* **1998,** *16*, 3295–3300.

(12) Marchenko, A.; Xie, Z. X.; Cousty, J.; Van, L. P. *Surf. Interface Anal.* **2000,** *30*, 167–169.

(13) Xie, Z. X.; Huang, Z. F.; Xu, X. *Phys. Chem. Chem. Phys.* **2002,** *4*, 1486–1489.

(14) Yasuda, S.; Shigekawa, H. *Jpn. J. Appl. Phys., Part 1* **2003,** *42*, 4901–4904.

(15) Katsonis, N.; Marchenko, A.; Fichou, D. *J. Am. Chem. Soc.* **2003,** *125*, 13682–13683.

(16) Clavilier, J.; Faure, R.; Guinet, G.; Durand, R. *J. Electroanal. Chem.* **1980,** *107*, 205–209.

(17) Yamada, R.; Uosaki, K. *J. Phys. Chem. B* **2000,** *104*, 6021–6027.

(18) He, Y. F.; Ye, T.; Borguet, E. *J. Phys. Chem. B* **2002,** *106*, 11264–11271.

(19) Xu, S. M.; Szymanski, G.; Lipkowski, J. *J. Am. Chem. Soc.* **2004,** *126*, 12276–12277.

(20) Xie, Z. X.; Xu, X.; Tang, J.; Mao, B. W. *J. Phys. Chem. B* **2000,** *104*, 11719–11722.

(21) Marchenko, A.; Cousty, J.; Van, L. P. *Langmuir* **2002,** *18*, 1171–1175.

(22) Zhang, H. M.; Xie, Z. X.; Mao, B. W.; Xu, X. *Chem.—Eur. J.* **2004,** *10*, 1415–1422.

(23) Zhang, H. M.; Yan, J. W.; Xie, Z. X.; Mao, B. W.; Xu, X. *Chem.—Eur. J.* **2006,** *12*, 4006–4013.

(24) Ishikawa, Y.; Ohira, A.; Sakata, M.; Hirayama, C.; Kunitake, M. *Chemical Communications* **2002**, *22*, 2652–2653.

(25) Su, G. J.; Zhang, H. M.; Wan, L. J.; Bai, C. L.; Wandlowski, T. *J. Phys. Chem. B* **2004,** *108*, 1931–1937.

(26) Plass, K. E.; Kim, K.; Matzger, A. J. *J. Am. Chem. Soc.* **2004,** *126*, 9042–9053.

(27) Tahara, K.; Furukawa, S.; Uji-I, H.; Uchino, T.; Ichikawa, T.; Zhang, J.; Mamdouh, W.; Sonoda, M.; De Schryver, F. C.; De Feyter, S.; Tobe, Y. *J. Am. Chem. Soc.* **2006,** *128*, 16613–16625.

(28) Yan, H. J.; Lu, J.; Wan, L. J.; Bai, C. L. *J. Phys. Chem. B* **2004,** *108*, 11251–11255.

(29) Ruben, M.; Payer, D.; Landa, A.; Comisso, A.; Gattinoni, C.; Lin, N.; Collin, J. P.; Sauvage, J. P.; De Vita, A.; Kern, K. *J. Am. Chem. Soc.* **2006,** *128*, 15644–15651.

(30) Laibinis, P. E.; Whitesides, G. M. *J. Am. Chem. Soc.* **1992,** *114*, 1990–1995.

(31) Bain, C. D.; Evall, J.; Whitesides, G. M. *J. Am. Chem. Soc.* **1989,** *111*, 7155–7164.

(32) Sellers, H.; Ulman, A.; Shnidman, Y.; Eilers, J. E. *J. Am. Chem. Soc.* **1993,** *115*, 9389–9401.

(33) Kern, H. E. P., A.; Brauer, U.; Findenegg, G.H. *Progress in Colloid and Polymer Science* **1978,** *65*, 118–124.

(34) Streitwieser, A.; Heathcock, C. H.; Kosower, E. M. *Introduction to Organic Chemistry*, 4th ed.; Prentice-Hall Inc: Upper Saddle River, NJ, 1992; p 810.

(35) Parker, A. J. “Sulfur Nucleophiles in Aromatic SN Reactions.” In *Organic Sulfur Compounds;* Kharasch, N., Ed.; Pergamon Press: New York, 1961; Vol. 1, p 103.

(36) Harten, U.; Lahee, A. M.; Toennies, J. P.; Woll, C. *Phys. Rev. Lett.* **1985,** *54*, 2619–2622.

(37) Lackinger, M.; Griessl, S.; Heckl, W. A.; Hietschold, M.; Flynn, G. W. *Langmuir* **2005,** *21*, 4984–4988.

(38) Uemura, S.; Sakata, M.; Taniguchi, I.; Kunitake, M.; Hirayama, C. *Langmuir* **2001,** *17*, 5–7.

(39) Heben, M. J.; Dovek, M. M.; Lewis, N. S.; Penner, R. M.; Quate, C. F. *Journal of Microscopy—Oxford* **1988,** *152*, 651–661.

(40) Heben, M. J.; Penner, R. M.; Lewis, N. S.; Dovek, M. M.; Quate, C. F. *Appl. Phys. Lett.* **1989,** *54*, 1421–1423.

(41) Heben, M. J. “Scanning Tunneling Microscopy in Electrochemical Environments.” *Ph.D. Thesis*, California Institute of Technology, February 1990.